Video Article

Non-aqueous Electrode Processing and Construction of Lithium-ion Coin Cells

Malcolm Stein IV[1], Chien-Fan Chen[1], Daniel J. Robles[1], Christopher Rhodes[2], Partha P. Mukherjee[1]

[1]Department of Mechanical Engineering, Texas A&M University

[2]Department of Chemistry and Biochemistry, Texas State University

Correspondence to: Partha P. Mukherjee at pmukherjee@tamu.edu

Abstract

Research into new and improved materials to be utilized in lithium-ion batteries (LIB) necessitates an experimental counterpart to any computational analysis. Testing of lithium-ion batteries in an academic setting has taken on several forms, but at the most basic level lies the coin cell construction. In traditional LIB electrode preparation, a multi-phase slurry composed of active material, binder, and conductive additive is cast out onto a substrate. An electrode disc can then be punched from the dried sheet and used in the construction of a coin cell for electrochemical evaluation. Utilization of the potential of the active material in a battery is critically dependent on the microstructure of the electrode, as an appropriate distribution of the primary components are crucial to ensuring optimal electrical conductivity, porosity, and tortuosity, such that electrochemical and transport interaction is optimized. Processing steps ranging from the combination of dry powder, wet mixing, and drying can all critically affect multi-phase interactions that influence the microstructure formation. Electrochemical probing necessitates the construction of electrodes and coin cells with the utmost care and precision. This paper aims at providing a step-by-step guide of non-aqueous electrode processing and coin cell construction for lithium-ion batteries within an academic setting and with emphasis on deciphering the influence of drying and calendaring.

Video Link

The video component of this article can be found at https://www.jove.com/video/53490/

Introduction

Lithium-ion batteries represent a promising source to fulfill the ever increasing requirements of energy storage devices[1-4]. Improvements in the capacity of LIBs would not only improve the effective range of electric vehicles[5,6], but also improve their cycle life by reducing the depth of discharge, which in turn increases the viability of LIBs for use in grid energy storage applications[7].

Originally used for hearing aids in the 1970s[8], coin cells today are commonly used in the development and evaluation of new and existing electrode materials. As one of the smallest form factors for batteries, these cells represent a simple and effective way to create batteries in an academic research setting. A typical Lithium-Ion battery consists of a cathode, anode, current collectors, and a porous separator that prevents shorting of the anode and cathode. During the operation of a Lithium-Ion battery, ions and electrons are mobile. During discharge, ions travel from the negative electrode (anode) through the porous separator and into the positive electrode, or cathode. Meanwhile, electrons travel through the current collector, across the external circuit, finally recombining with the ions on the cathode side. In order to reduce any resistances associated with ion and electron transfer, the components need to be properly oriented — the distance ions travel should be minimized. Typically these components are combined a "sandwich" configuration. Batteries used in electric vehicles, cell phones, and consumer electronics consist of large sandwiches that are spirally wound or folded, depending on the form factor of the battery. These types of cells can be very difficult to manufacture on small scales without incurring high costs. However, in a coin cell there is only a single sandwich within the cell. Although specialized equipment is still necessary to create the electrodes in coin cells, the cells themselves can be quickly assembled by hand and sealed within a controlled environment.

The performance of batteries, regardless of type, is dependent on the materials that form the positive and negative electrode, the choice of electrolyte, and the cell architecture[4,9-13]. A typical LIB electrode is composed of a combination of Li-containing active material, conductive additive, polymeric binder, and void space that is filled with an electrolyte. Electrode processing can be organized into five main steps: dry powder mixing, wet mixing, substrate preparation, film application, and drying — a step that is often given little attention. When producing an electrode using these processing steps, the end goal is to achieve a uniform electrode film consisting of the active material, conductive additive, binder. This uniform distribution is critical to optimal performance of LIBs[14-18].

This guide represents the steps utilized at Texas A&M in the Energy and Transport Sciences Laboratory (ETSL) and at Texas State University to manufacture coin cells for the evaluation of new and existing electrode materials. Beyond the basic steps found documented in many sources,

we have included our own expertise at critical steps, noting important details that are often left out of similar methods documents and many publications. Additionally, the primary physical and electrochemical methods utilized in our lab (galvanostatic cycling and Electrochemical Impedance Spectroscopy (EIS)) are elucidated within.

Protocol

Caution should be exercised when using any of the solvents, reagents, or dry powders utilized in this protocol. Read all MSDS sheets and take appropriate safety measures. Standard safety equipment includes gloves, safety glasses, and a lab coat.

1. Cathode Preparation

Note: The schematic overview of the cathode fabrication process is presented in **Figure 1**.
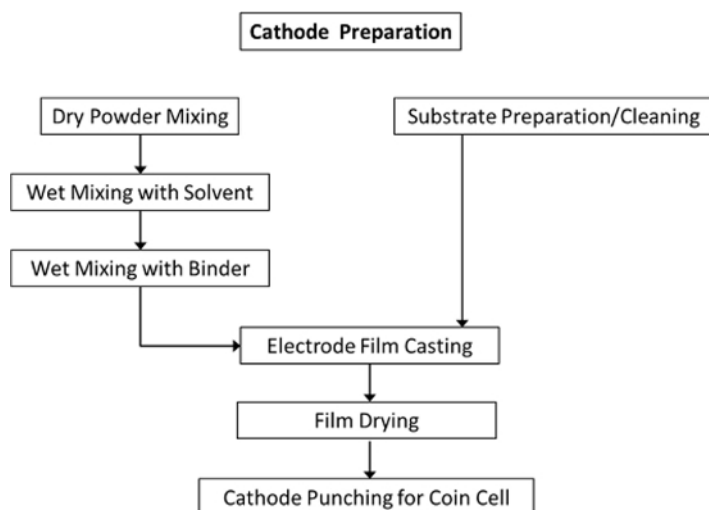
Figure 1. Schematic overview of the steps utilized in the ETSL to create cathodes. The main process includes preparation and casting of the electrode slurry onto a cleaned aluminum substrate, followed by drying of the electrode sheet and incorporation into coin cells. Please click here to view a larger version of this figure.

1. **Aluminum Substrate Preparation**
    1. Cut a 4.5" by 12" sheet of 15 μm thick aluminum (Al) foil using a paper cutter or scissors.
    2. Spray acetone on the surface of a clean plastic board to adhere the foil to the board and then place the foil sheet onto the board.
    3. Spray a generous amount of acetone on the surface of the foil and begin to scrub the entire surface using a scotch pad with small semi-circle motions. Spray additional acetone on the surface and wipe down residue with a paper towel.
    4. Repeat steps 1.1.2-1.1.3 for the opposite side and then repeat once more for the casting side.
    5. Wash etched Al sheet with deionized (DI) water on casting side first, then flip and repeat with opposite side. Re-scrub the surface of the Al foil as the DI water displays poor wettability and does not flow off the surface of the sheet without forming droplets. Repeat rinsing with isopropyl alcohol.
    6. Transfer the cleaned Al sheet between two paper towels and allow to dry for approximately 20 min under compression between two flat planes and paper towels.

2. **Slurry Preparation**
    1. Choose the weights of active material, conductive additive and binder based on the desired composition of the electrode sheet. Choose a total dry powder weight of 1.25 g, with 70 wt% lithium-manganese-cobalt-oxide, $LiNi_{1/3}Mn_{1/3}Co_{1/3}O_2$ (NMC, active material), 20 wt% carbon black (conductive additive) and 10% Polyvinylidene Difluoride (PVDF, binder).
    2. Measure out 0.875 g of NMC and 0.25 g of carbon black and place into an agate mortar and pestle. Lightly mix the materials together without grinding. After a mixture starts to form, mill by hand in the mortar and pestle for 3-5 min, until a uniform powder is visually observed.
    3. Transfer the mixed powder into a disposable mixing tube with a piece of weigh paper. Add 16 glass balls (6 mm diameter) to the powder, along with 5.5 ml of 1-methyl-2-pyrrolidinone (NMP), the non-aqueous solvent.
    4. Place the disposable tube onto the tube drive station and lock into place. Turn the drive on and slowly increase to the maximum speed. Allow contents to mix for 15 min.
    5. Add 1.25 g of a 10% PVDF in NMP solution directly to the tube. Place the tube back onto the drive and allow mixing for 8 min, following the same procedure in 1.2.4. If the tube is allowed to sit for more than 5 min prior to casting (below), mix the contents for an additional 15 min.

3. **Casting and Drying**
    1. Clean the metal surface of the automatic film applicator with isopropyl alcohol and a paper towel. Ensure that the doctor blade is clean, and is set to the desired casting height (200 μm).

2. Apply a layer of isopropyl alcohol to the surface of the film applicator and place the dried aluminum substrate shiny-side down onto the surface. Press out the excess isopropyl alcohol with a folded paper towel until all wrinkles and isopropyl are removed. Take care to avoid tearing the substrate by firmly holding one of the substrate in place.

3. Remove the mixing tube from the tube drive and open the container. Pour the slurry onto the surface of the substrate in a 2-3 inch line approximately 1 inch from the top (initial casting side) of the substrate. Remove any glass balls from the sheet with clean metallic tweezers.

4. Set the casting speed to 20 mm/sec, and activate the casting arm of the film applicator.

5. Lift the cast electrode from the surface of the film applicator using a thin piece of cardboard to ensure no wrinkles form on the sheet.

6. Allow the electrode sheet to dry for 16 hr at RT (~24 °C) followed by drying at 70 °C for ~3 hr or until the sheet is dry. Ensure that the electrode is environmentally isolated in a fume hood or sealed chamber to prevent non-uniform drying.

4. **Cathode Electrode Punching**
   1. Place the dried electrode sheet onto a cleaned sheet of aluminum metal. Take out a ½" hole punch and place it gently onto a region of the sheet with a uniform surface (edges may appear non-uniform). Slowly apply pressure to the punch (by hand) and "roll" the pressure around the edges of the punch to ensure a clean cut.
   2. (Alternative) Cut out an electrode disc utilizing a precise disc cutter in lieu of manual punching.
   3. Remove the electrode from the sheet with cleaned, plastic tweezers and place it into a labeled vial, with the electrode surface facing up. Repeat twice.
   4. (Optional) Place a punched electrode onto the surface of the lab press. Apply pressure of roughly 4 MPa (the optimal pressure will vary based on the press utilized). Repeat for the remaining electrodes.
   5. Place the vials in a vacuum oven and allow the electrodes to further dry at 120 °C at -0.1 MPa for 12 hr to remove any remaining moisture. After, remove the electrodes and weigh them within 0.0001 g.
   6. Open the antechamber of the glovebox and place the vials onto the tray. Close the chamber the door and ensure a tight seal by using two fingers to tighten antechamber hatch.
   7. Bring the vacuum down to -0.1 MPa, and then fill with Argon. Repeat this process 1-2 more times, depending on the samples transported into the glovebox.

2. Anode Sheet for Full Cell

1. Repeat section 1 except using 9 µm thick copper foil as the substrate instead of aluminum foil. The composition of the sheet may be altered to fit specific needs.

3. Coin Cell Pre-assembly

Caution: The construction of coin cells is performed within an inert (Argon) environment within a glovebox. Extreme caution must be taken to minimize exposure of the internal environment to external atmosphere. Work with sharp materials within the glovebox should be minimized if possible. As a general rule, a task within the glovebox should take 3 times longer than the speed at which the task would be performed outside. Gloves should also be worn over the glovebox gloves to minimize exposure when working with different substances.

Note: The components needed for the construction of the coin cell, including the cap, case, wave springs, gaskets, spacers, lithium ribbon, electrolyte and remaining tools such as plastic tweezers (for component placement) are contained within an Argon-filled glovebox with O_2 and H_2O levels maintained below 0.5 parts per million. All components inserted into the glovebox (including lint-free task wipes) should be heated O/N in a vacuum oven at 120 °C at a pressure of -0.1 MPa to remove any moisture.

1. **Counter-electrode Preparation**
   1. Within the glovebox, remove lithium ribbon (0.75 mm thick) from sealed container and roll out a portion onto the surface of a plastic block. Using a razor blade, carefully scrape away any black-colored oxidation from the foil surface. Take extreme caution to avoid cutting the gloves.
   2. Take a 9/16" hole punch and punch out a disk of the lithium ribbon. Use a finger (separated from the lithium by rubber gloves within glovebox) or other blunt tool to push the lithium disk out of the punch.
   3. Take a 0.5 mm thick spacer and gently apply the lithium disc to the surface between fingers. Ensure the lithium disc sticks to the center of the spacer and is flat — an uneven surface can cause uneven current distributions.

2. **Electrolyte Preparation**
   1. Store the electrolyte of choice (in this case 1 M $LiPF_6$ in EC/DEC 1:1 by vol) within the glovebox at all times in an aluminum container, as the electrolyte is photosensitive.
   2. Remove a small amount of electrolyte from the source container into a working container.

3. **Celgard Separator Preparation**
   1. Place a sheet of the separator membrane between a folded sheet of printer paper. Place the folded paper and membrane onto a sheet of aluminum metal.
   2. Place a cushioning layer on top of the hole punch and use a hammer to punch out a ¾" diameter separator membrane.
   3. Transfer the punched separator discs into the glovebox utilizing the procedures outlined in 1.4.6-1.4.7.
      Note: It is recommended to perform this step in bulk to avoid having to punch out individual separators for each coin cell being constructed.

4. Coin Cell Assembly

Note: The configuration of the coin cell is presented in **Figure 2**.
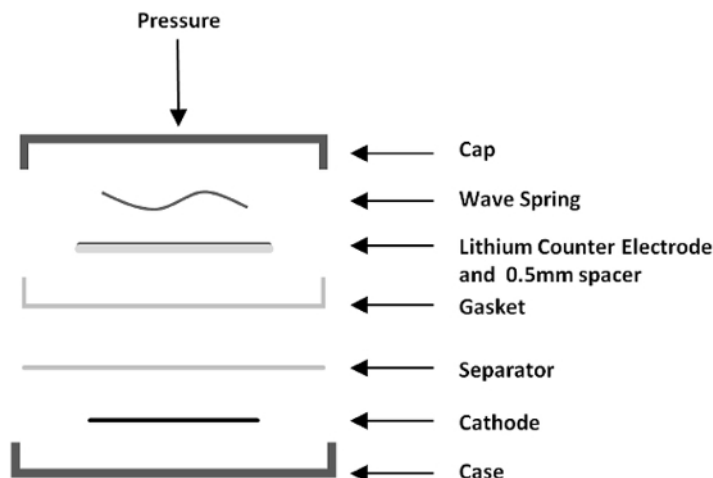
Figure 2. Coin cell components displayed in order of placement within cell. Placement of the cathode is followed by the separator, gasket, counter electrode and wave spring, followed by sealing of the cell. Please click here to view a larger version of this figure.

1. Open the interior antechamber door. Pull any components within the antechamber into the glovebox and reseal the interior antechamber door.
2. Place a coin cell case into a small weigh boat. Place the cathode into the center of the coin cell case. Apply 1-2 ~30 µl drops of electrolyte to the center of the electrode and apply 1 drop on opposite sides of the rim of the case.
3. Place a single ¾" separator onto the surface of the electrode. Force out any bubbles that become trapped using the flat edge of a pair of tweezers, and re-center the cathode by grabbing the case by the lip and lightly tapping the electrode into place. Apply an additional 1-2 drops of electrolyte to allow for better movement of the electrode if it sticks to its original position.
4. Place the gasket into the case, with the flat side facing down and the lipped side facing up. Confirm the orientation of the gasket by holding up to the light prior to cell insertion.
5. Apply 2-3 ~30 µl drops of electrolyte to the center of the cell, and place the prepared counter electrode onto the center with the lithium facing down. Place the wave spring on top of the centered counter electrode.
6. Fill the cell to the brim (~0.7 ml) with electrolyte until it forms a curved, convex meniscus that covers most of the wave spring surface.
7. Carefully place the coin cell cap on top of the cell utilizing the tweezers to hold the cap centered vertically over the cell. Take care to center the cap to avoid excessive loss of electrolyte.
8. Press down on the cap (by hand) until it sets into the lip of the gasket. Transfer the cell to the crimper and ensure that the cell is centered in the groove of the crimping die. Crimp the cell to a pressure of ~ 6.2 MPa (900 psi) and release.
9. Remove the cell from the crimper (by hand), and clean off any excess electrolyte. Repeat steps 4.2- 4.9 until all desired cells are constructed. Clean any spilled electrolyte, place trash into an appropriate container. Transfer the cells out of the glovebox and label them.

5. Electrochemical Evaluation

1. Connect the cleaned cells to the battery cycler. Ensure the terminals are correctly connected by measuring the open circuit potential. If not positive, reverse the connections.
2. Calculate the desired current based on the weight of the dried electrode on the surface of the aluminum substrate, the known mass of the aluminum, the active material percentage by weight, and the rated specific capacity of the active material utilized.
   1. With a measured electrode mass of 0.0090 g, aluminum disc mass of 0.0054 g, and rated capacity of 155 mAh/g, determine the desired current as (0.0090 g - 0.0054 g) × 0.70 × 155 mAh/g = 0.3906 mAh. For discharge at the current required to fully discharge the cell in 1 hr (1C), the applied current is 0.3906 mA.

3. Set the schedule on the cycler to charge/discharge the cell between the upper and lower voltage levels of 4.2 V and 2.8 V. Cycle the cell 4 times at a rate of C/10 (galvanostatic, constant current). Then charge the cell once at C/10.
4. After the 5th C/10 charge, remove the cell from the cycler (if necessary) and perform Electrochemical Impedance Spectroscopy[19] (EIS) on the cell, after resting for 1 hr. Place the cell back on the cycler and discharge at C/10. Perform EIS once more after resting for 1 hr.
5. Place the cell back onto the cycler and cycle the cell 5 times at rates of C/5, C, 2C, 5C, and 10C, followed by 100 1C cycles.
6. Determine the specific capacity of the cells at each C-rate by dividing the capacity in mAh by the mass of active material present in the cathode. Calculate the capacity retention by dividing the average specific capacity of the last 5 1C cycles by the average specific capacity of the first 5 1C cycles.

Representative Results

A properly cast electrode sheet should appear uniform in surface appearance and properly adhere to the current collector. Typically flaking of the electrode sheet is caused by either poor etching of the substrate, or having to little NMP in the initial mixing stage. Alternatively, too much NMP can cause the sheet to display a higher degree of porosity, which is not desirable. Lastly, a third pattern can be observed on the electrode surface, where pooling appears to occur. Interactions with the ambient conditions of the room (humidity, temperature, and any air movement) are the most likely causes for this behavior. Isolation within a fume hood can prevent this behavior. These scenarios can be seen in **Figure 3**.

The coin cell should appear as shown in **Figure 4**, with no broken edges. When the cell is not properly sealed, exposure to the atmosphere will cause swelling of the lithium, which will cause the cell to pop open. It is also possible to crush the cell when crimping. To prevent this the crimping pressure needs to be optimized for the chosen crimper and cell components.

Scanning electron microscope (SEM) imaging of the electrode surface (**Figure 5**) reveals the complexity of a cathode utilized in the construction of a coin cell. The large particles shown are the active material. The remaining material is a combination of PVDF and carbon black.

The structure itself is stochastic in nature, but proper processing influences the distribution of particles within the sheet. Drying can cause a poor distribution of binder and conductive additive that can negatively affect cell performance. Shown in **Figure 6** are representative cycling results for a sheet that was dried too fast and a sheet that was properly dried utilizing the two-stage process presented.

This cycling data allows us to view the performance (in terms of specific capacity) of the cells at various rates, and allows us to look at capacity retention after extended cycling. Discharge curves such as those shown in **Figure 7** can be utilized to view the specific energy of the cells, which is determined as the area underneath the discharge curve.

The EIS data for the cells under consideration can be used to further characterize the cells. A representative EIS spectrum can be seen in **Figure 8**.

When comparing EIS spectra, two primary components (for a discharged cell) are the (i) high frequency semicircle, and (ii) the low frequency tail. The slope of the tail indicates resistance due to diffusion, and the semicircle represents a number of resistances due to charge transfer resistance, and several other contributions, depending on the frequency range. In the case of the differently dried electrodes, the quickly dried sheet has a larger radius indicating higher charge transfer resistance.

Representative results for the impact of porosity and electrode thickness are additionally shown below in **Figure 9**.

A thinner sheet allows for shorter diffusion distances, and the porosity can be optimized to additionally allow for more efficient transfer. It is important, however, to recognize that these parameters are not absolute, as tradeoffs will exist[19,20]. The casting thickness, slurry viscosity and composition, and the degree of calendaring all have a direct impact on the porosity and thickness of a sheet. Thus by carefully manipulating the steps outlined in this document, microstructural characteristics can be controlled.
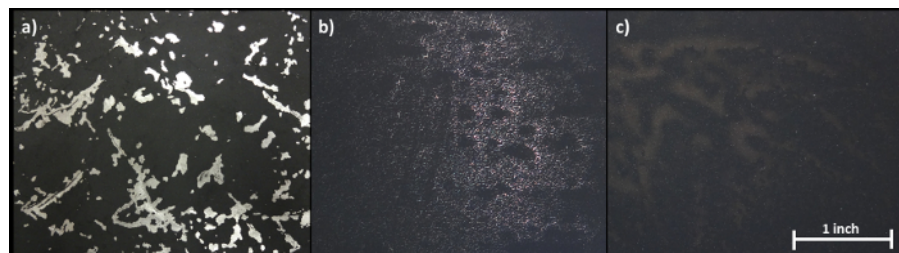

Figure 3. Electrode sheets: (A) with too little NMP, (B) with too much NMP, and (C) with non-uniform drying. Each condition results in poor mechanical stability and reduced electrochemical performance as a result. Typically flaking of the electrode sheet is caused by either poor etching of the substrate, or having to little NMP in the initial mixing stage (a). Alternatively, too much NMP can cause the sheet to display a higher degree of porosity, which is not desirable (b). Lastly, an non-uniform surface can appear that is similar in appearance to material pooling during drying (c). Please click here to view a larger version of this figure.

Figure 4. Coin cell that has been properly crimped (left) and improperly crimped (right). An improperly crimped cell will be noticeably open immediately after crimping or can pop over several hours later. Please click here to view a larger version of this figure.
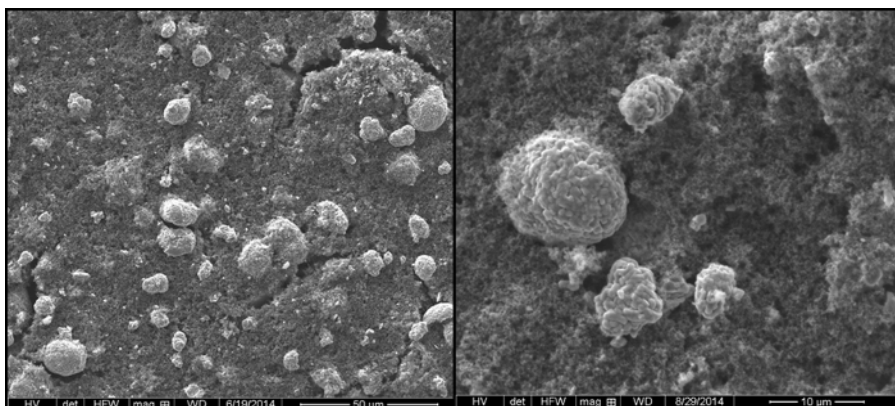

Figure 5. SEM image of the surface of uncalendered NMC cathode. The active material (NMC) can be seen as the large spherical particles (~10 µm diameter) with the binder/additive (PVDF/carbon black) composite surrounding the active material particles. The scale for the left image is 50 µm and is the right is 10 µm. Please click here to view a larger version of this figure.
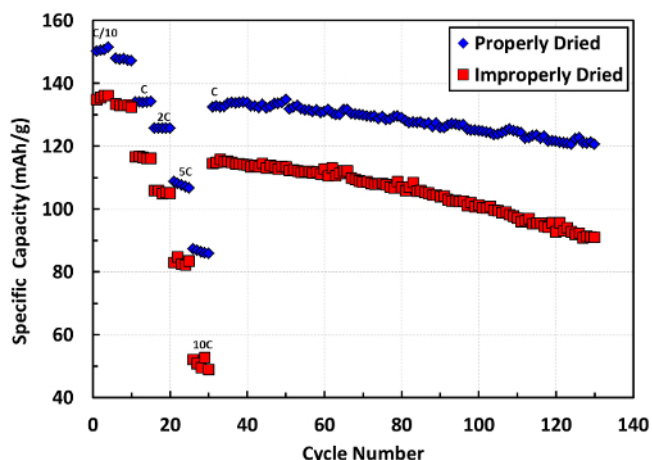

Figure 6. Cycling data shown for an electrode dried too quickly (improperly) and a lower rate utilizing a two-stage dry. The specific capacity of the cells at rates of C/10, C/5, C, 2C, 5C, and 10C followed by long-term cycling at 1C. The cells were cycled at RT (~22 °C) with cells consisting of NMC - Li cells with the material loadings depicted in the protocol. C-rate is determined with respect to the rated capacity of the NMC, approximately 150 mAh/g. Please click here to view a larger version of this figure.
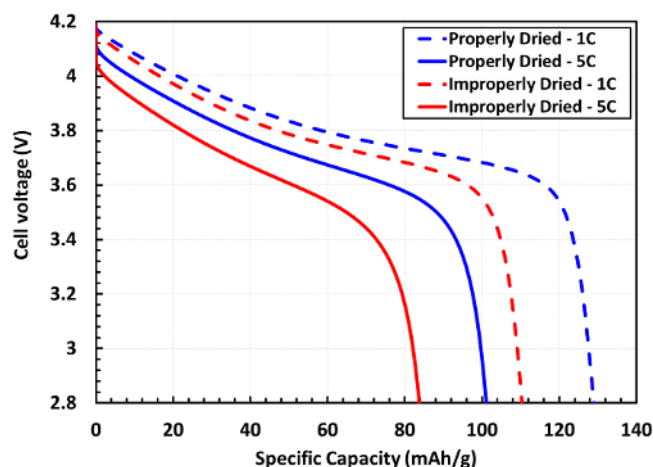
Figure 7. Discharge curve shown for an electrode dried too quickly (improperly) and a lower rate utilizing a two-stage dry. The discharge curves for rates of 1C and 5C are shown. The specific energy of the cell can be determined as the area underneath the discharge curve. Please click here to view a larger version of this figure.
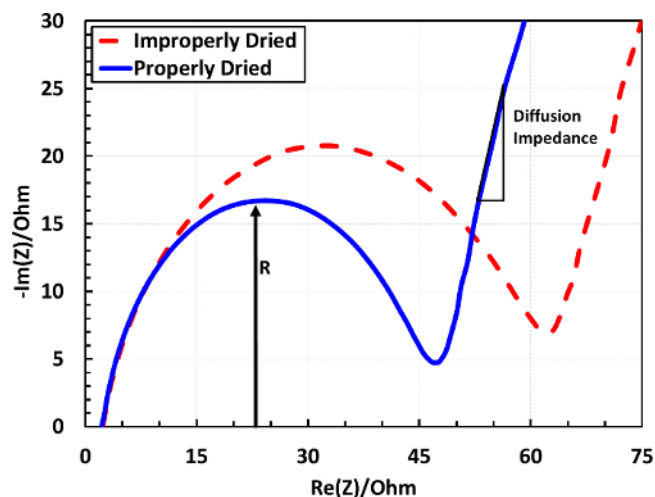
Figure 8. Example EIS spectrum for a scanning frequency range of 1 MHz to 100 mHz. Data is shown after the 5th C/10 discharge for the same cases presented in **Figures 7** and **8**. Please click here to view a larger version of this figure.
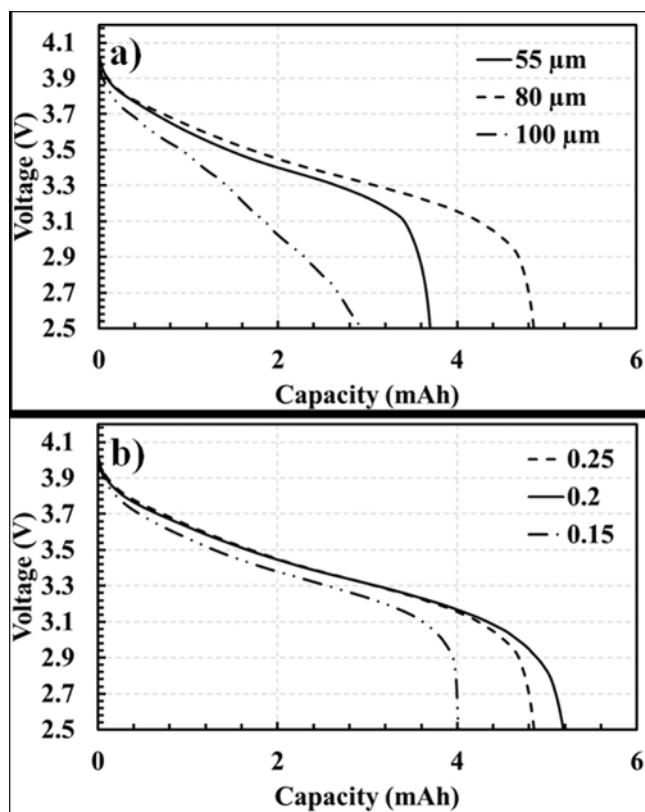
Figure 9. Impact of electrode thickness (A) and porosity (B) on discharge performance. Each of these parameters can be altered by controlling the steps discussed in this technique (calendering, casting thickness, slurry viscosity, *etc.*). Please click here to view a larger version of this figure.

Discussion

The optimization of the wet mixing stages are crucial to the slurry viscosity and coating ability, which impacts the uniformity and adhesion of the electrode. Here a high-shear mixing method is utilized, where the solvent, additive, binder, and active material are mixed together utilizing the kinetic motions of the glass balls present in the vials. This mixing technique offers the benefit of much more rapid mixing times as compared to a magnetic stirrer method. Beyond this, this high shear mixing allows for more viscous solutions to be effectively mixed, and provides the energy necessary to mix more difficult binders such as xanthan gum in water. As the abrasive nature of the mixing can cause glass impurities to mix into the electrode slurry, used glass balls should be discarded so as to minimize this effect. The minimum quantity of glass balls needed is dependent on the mixing ability of the components within the vial. However, an upper limit exists due to the loss of slurry coating the glass balls after mixing. With too little slurry or too many balls, it will not be possible to extract enough of the electrode slurry to cast an electrode. The amount of NMP required is based on the total surface area of the particles present in the dry mixture[21]. For example, if the desired dry weight ratio of components was adjusted to include 10% carbon black as opposed to 20% (with 80% NMC and 10% PVDF), a significantly lower amount of NMP would be required: 2.0 ml (with a dry powder mass of 1 g). Further, with a composition of 94% active material, 3% conductive additive and 3% binder, 1.5 ml of NMP is required (again with 1 g dry powder mass). This owes primarily to the fact that the Brunauer-Emmet-Teller (BET) surface area of carbon black is much higher than that of the remaining components. Thus the determination of the appropriate solvent content in the initial mixing stage must be carefully determined when working with new desired sheet compositions. The ideal observed viscosity for the composition noted herein is 0.11 Pa·sec. It should be noted that the composition of the electrode sheet utilized should be adjusted to fit the specific needs and performance of the materials utilized. Typically, a higher active material content is utilized to reduce the amount of inactive material present in electrodes. However tradeoffs exist in terms of cell performance at increased rates.

Even with a perfect slurry it is possible to obtain a bad electrode sheet due to the adhesion to the current collector. During the manufacturing process, the aluminum foil is coated with a thin layer of oil to prevent self-adhesion when rolling the material. If not properly cleaned, this remaining residue will reduce the electrode adhesion. During cleaning, extra emphasis should be taken towards ensuring the cleanliness of the electrode substrate. The order in which the sheet is cleaned (casting side, then button side, followed by casting) is to ensure that the casting surface is as clean as possible. Care should be taken to use paper towels that are soft enough (and sufficiently free of lint) such that the surface of the current collector is not deformed and remains free of surface pitting. The electrode flaking displayed in **Figure 3A** is representative of the resulting adhesion from utilizing an improperly cleaned substrate. This could occur from not scrubbing enough (and thus resulting in poor wettability) or scrubbing too hard (which can result in visually observable pitting of the substrate surface). The etching method utilized here is sufficient for good adhesion with the non-aqueous solvent and binder utilized. Different binders and solvent might require alternative methods to achieve adhesion, such as corona discharge or pre-heat treatment of the current collector. For example, although the flow of DI water over the surface of the electrode with minimal recession and low wetting angle indicates a sufficient casting surface, the provided wettability is not sufficient for aqueous processing.

A step that is often paid little attention is electrode drying. Here the final microstructure of the cell is set as the solvent evaporates. The vertical migration of mobile electrode constituents (binder and additive) can cause a vertical distribution of these materials to develop[22]. In practice, rapid evaporation of the solvent from the electrode surface results in the deposition of concentrated binder (present in the liquid solution of solvent) and carbon (the conductive additive) at the surface of the electrode. Although this effect occurs at any drying speed, at higher rates there is not sufficient time for the redistribution of these components via diffusion. The two-stage drying process allows for uniform evaporation of the free solvent, followed by the evaporation of solvent trapped inside the microstructure during the oven drying stage.

When constructing the coin cell, care must be taken to ensure that the anode and cathode are carefully aligned within the cell. Here, a slightly larger diameter anode is utilized to allow for a margin of error in placement. The spacer and wave spring within the cell serve to increase the thickness of the internal components such that a complete circuit is formed. Also critical to this circuit is the electrolyte, through which the Lithium-ions travel. With the given form factor a large amount of empty space exists within the cell. Thus it is possible to have an uneven amount of electrolyte present within the cell. Fully soaking the cell ensure no or minimal pockets of argon exists that can upset the distribution of electrolyte in the sandwich.

During electrochemical characterization, either galvanostatic (which is utilized here) or potentiostatic cycling can be utilized. During galvanostatic charge/discharge the current is maintained constant and the cell is deemed as charged or discharged after reaching an upper or lower potential limit. This potential limit is dependent on the active material utilized. Charging or discharging the active material beyond these limitations can result in degradation. During potentiostatic charge/discharge the voltage is maintained constant, while the current varies. One drawback of potentiostatic cycling is the additional time required for the current to drop off to the lower limit. This and the desired cycling rates will need to be configured based on the desired information and materials utilized. The protocol listed herein is a general purpose protocol, but may not suit all needs.

This technique offers a method for the creation of electrode sheets and coin cells in a precisely controlled manner that is suitable for reproduction in academic or industrial research setting. The fundamentals of this technique can be utilized as the basis for creating electrode sheets for larger battery form factors, aqueous processing, and various cell chemistries and compositions, although specific stage might need to be optimized. This technique is limited to the creation of customized electrodes (positive or negative) where the final distribution of materials (although perhaps uniform within the domain) is stochastic. Additionally, the creation of cells with larger form factors would require modifications to the electrode size produced (larger casting sheet) and the cell components utilized.

Disclosures

The authors have nothing to disclose.

Acknowledgements

References

1. Wagner, R., Preschitschek, N., Passerini, S., Leker, J., & Winter, M. Current research trends and prospects among the various materials and designs used in lithium-based batteries. *J Appl Electrochem.* **43**, 481-496 (2013).
2. Whittingham, M. S. Lithium batteries and cathode materials. *Chem Rev.* **104**, 4271-4301 (2004).
3. Ellis, B. L., Lee, K. T., & Nazar, L. F. Positive Electrode Materials for Li-Ion and Li-Batteries. *Chem Mater.* **22**, 691-714 (2010).
4. Tarascon, J. M., & Armand, M. Issues and challenges facing rechargeable lithium batteries. *Nature.* **414**, 359-367 (2001).
5. Smith, K., & Wang, C. Y. Power and thermal characterization of a lithium-ion battery pack for hybrid-electric vehicles. *J Power Sources.* **160**, 662-673 (2006).
6. Lu, L. G., Han, X. B., Li, J. Q., Hua, J. F., & Ouyang, M. G. A review on the key issues for lithium-ion battery management in electric vehicles. *J Power Sources.* **226**, 272-288 (2013).
7. Dunn, B., Kamath, H., & Tarascon, J. M. Electrical Energy Storage for the Grid: A Battery of Choices. *Science.* **334**, 928-935 (2011).
8. Cich, ER. inventor; Esb Inc, assignee. *Button Cell battery.* US patent. 3,655,452A. Apr 11 (1972).
9. Elul, S., Cohen, Y., & Aurbach, D. The influence of geometry in 2D simulation on the charge/discharge processes in Li-ion batteries. *J Electroanal Chem.* **682**, 53-65 (2012).
10. Buqa, H., Goers, D., Holzapfel, M., Spahr, M. E., & Novak, P. High rate capability of graphite negative electrodes for lithium-ion batteries. *J Electrochem Soc.* **152**, (2005).
11. Chen, Y. H., Wang, C. W., Zhang, X., & Sastry, A. M. Porous cathode optimization for lithium cells: Ionic and electronic conductivity, capacity, and selection of materials. *J Power Sources.* **195**, 2851-2862 (2010).
12. Arora, P., Doyle, M., Gozdz, A. S., White, R. E., & Newman, J. Comparison between computer simulations and experimental data for high-rate discharges of plastic lithium-ion batteries. *J Power Sources.* **88**, 219-231 (2000).
13. Dillon, S. J., & Sun, K. Microstructural design considerations for Li-ion battery systems. *Curr Opin Solid St M.* **16**, 153-162 (2012).
14. Harris, S. J., & Lu, P. Effects of Inhomogeneities-Nanoscale to Mesoscale-on the Durability of Li-Ion Batteries. *J Phys Chem C.* **117**, 6481-6492 (2013).
15. Liu, G., Zheng, H., Song, X., & Battaglia, V. S. Particles and Polymer Binder Interaction: A Controlling Factor in Lithium-Ion Electrode Performance. *J Electrochem Soc.* **159**, A214-A221 (2012).
16. Zheng, H. H., Yang, R. Z., Liu, G., Song, X. Y., & Battaglia, V. S. Cooperation between Active Material, Polymeric Binder and Conductive Carbon Additive in Lithium Ion Battery Cathode. *J Phys Chem C.* **116**, 4875-4882 (2012).

17. Liu, Z. X., Battaglia, V., & Mukherjee, P. P. Mesoscale Elucidation of the Influence of Mixing Sequence in Electrode Processing. *Langmuir.* **30**, 15102-15113 (2014).

18. Liu, Z. X., & Mukherjee, P. P. Microstructure Evolution in Lithium-Ion Battery Electrode Processing. *J Electrochem Soc.* **161**, E3248-E3258 (2014).

19. Zheng, H. H., Tan, L., Liu, G., Song, X. Y., & Battaglia, V. S. Calendering effects on the physical and electrochemical properties of Li[Ni$_{1/3}$Mn$_{1/3}$Co$_{1/3}$]O^{-2} cathode. *J Power Sources.* **208**, 52-57 (2012).

20. Zheng, H. H., Li, J., Song, X. Y., Liu, G., & Battaglia, V. S. A comprehensive understanding of electrode thickness effects on the electrochemical performances of Li-ion battery cathodes. *Electrochim Acta.* **71**, 258-265 (2012).

21. Marks, T., Trussler, S., Smith, A. J., Xiong, D. J., & Dahn, J. R. A Guide to Li-Ion Coin-Cell Electrode Making for Academic Researchers. *J Electrochem Soc.* **158**, A51-A57 (2011).

22. Li, C. C., & Wang, Y. W. Binder Distributions in Water-Based and Organic-Based LiCoO$_2$ Electrode Sheets and Their Effects on Cell Performance. *J Electrochem Soc.* **158**, A1361-A1370 (2011).